Transport properties in multilayer adsorption of dimers

G. Palacios [1,*] L. A. P. Santos [1] and M. A. F. Gomes [2]
[1]*CNEN/CRCN-NE, 50740-545, Recife, PE, Brazil*
[2]*Departamento de Física, Universidade Federal de Pernambuco, 50670-901, Recife, PE, Brazil*

(Received 23 June 2022; accepted 22 August 2022; published 13 September 2022)

In this paper, we study the transport properties (percolation and conductivity) of a two-dimensional structure created by depositing dimers on a one-dimensional substrate where multilayer deposition is allowed. Specifically, we are interested in studying how the mentioned properties vary as a function of the height of the multilayer. The critical parameters of the percolation transition are calculated using finite-size scaling analysis, obtaining the scaling laws for the probability of percolation and the conductivity of the system. To calculate the electrical conductivity of the multilayer, we use the Frank-Lobb algorithm.

DOI: 10.1103/PhysRevE.106.034120

I. INTRODUCTION

A widely known and useful class of irreversible adsorption models that has attracted much attention in recent decades is random sequential adsorption (RSA), in which the units to be adsorbed, one at a time, cannot overlap with the previously adsorbed units [1]. The nonoverlap constraint can be eliminated and the new particle in the deposition queue becomes part of a new layer. In this case, we say that the adsorption is irreversible and multilayer.

Multilayer adsorption models present a greater resemblance to reality than monolayer-based models, depending on the type of interaction between the adsorbate and substrate, for example, to describe experiments with adhesion and reaction processes of colloidal particles and proteins at solid surfaces [2,3]. Correctly modeling multilayer adsorption allows us to describe the dynamics of various high-tech industrial processes such as the fabrication of multifunctional sensors [4–6]. It is also often used to model the dynamics of the formation of thin film materials [7].

In the last decades, there have been few relevant analytical results and numerical experiments that contribute to the understanding of the properties of the multilayer adsorption model. In general, the focus is on the study of the dynamics of the process. Analytical results were derived for the deposition of multilayers of dimers on a one-dimensional lattice within the rate equation approach [8]. However, the results are limited to the first two layers as the solution rapidly becomes cumbersome for high-layered structures. A general model of the irreversible multilayer deposition process that accounts for both surface screening and surface restructuring is presented in Ref. [9], but the analytical results are limited to the kinetics of the particle density in the first layer in one dimension when surface overhang rules are employed. A variant of the multilayer RSA process that is inspired by orthogonal resource sharing in wireless communication networks was developed in Ref. [10]. An approximation is presented here, based on the recursive approach that uses the results of monolayer RSA for indirect estimation of the density of rods for the multilayer version.

The study of transport properties in amorphous disordered systems is of great interest in different domains as those of theoretical [11] and experimental [12] physics, as well as in applied physics [13] and technology [14]. The transport properties in single-layer adsorption systems have been extensively studied with a focus on the dependence of the phenomenon on the density of adsorbed particles [15], of defects (sites where the adsorption is not allowed) [16], of the spatial distribution of the defects [17], and the anisotropy in the orientation of the adsorbed particles [18]. However, the applications are not just limited to single-layer systems. Ordered and disordered systems with a large number of layers of the order of tens or even hundreds of molecular layers have immense importance in theoretical and experimental physics and in current advanced technologies. They provide an opportunity to study the surface forces between microscopic adsorbed particles and between the surfaces of substrates and particles. They also attract interest that transcends basic physics, referring to such a diverse spectrum of applications from large-scale practical problems as flotation, water treatment, dyeing, soil science, microbiology, chemical catalysis to the interaction between cells, and other biological structures [19]. On the other hand, nanoconfined systems with tens to hundred of layers have impacted the commercial applications of polymeric structures [20]. From a more restricted physics perspective, the theoretical and experimental study of structures with many layers is important for understanding the behavior of several mechanical [21] and optical [22] properties, as well as for the understanding of the emergence of physical phenomena in semiconductor structures obtained with the use of molecular beam epitaxy techniques [23]. The results obtained in this paper show that transport properties such as percolation and conductivity begin to manifest when the system has many layers. This is undoubtedly an incentive to increase the interest of the community in exploring systems with a large number of layers.

*Corresponding author: palaciosg226@gmail.com

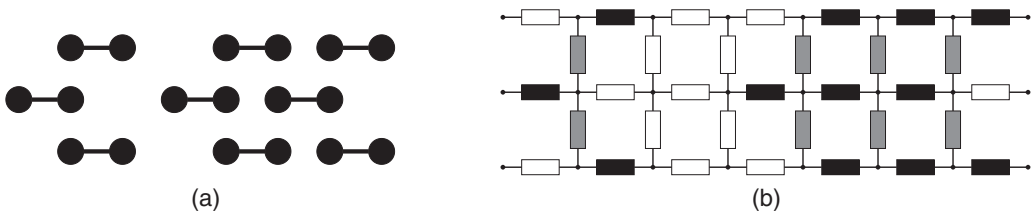

FIG. 1. (a) A portion of a square lattice filled by dimers with $L = 8$ and $H_{\max} = 3$ and (b) equivalent scheme of resistors. See text for details

Recently [10], there was a resurgence of interest in the study of multilayer adsorption, although until now there has been no study of the transport properties, e.g., percolation and conductivity in two-dimensional structures resulting from the one-dimensional multilayer packing process. Motivated by the growing need for the development of systems where transport properties are controlled, in this paper we report results of extensive numerical simulations of multilayer adsorption of dimers in a one-dimensional substrate where we calculate the critical parameters that characterize the aforementioned transport properties.

The structure of this paper is the following: In Sec. II, we introduce the numerical details of the simulations. In Sec. III, the results for percolation and conductivity are presented and discussed. We conclude in Sec. IV with a summary of the results and some prospects for future work.

II. DETAILS OF THE SIMULATION

The algorithm for deposition of dimers is incredibly simple since it does not have restrictions as is the case with the RSA algorithm, i.e., the dimer is always adsorbed. First, we draw a horizontal position $x_0 \in [1, L-1]$, then the dimer will be deposited occupying the sites $x = [x_0, x_0 + 1]$ at the height $y = h_{\max} + 1$, where $h_{\max}$ is the maximum height in the column $[x_0, x_0 + 1]$. Summarizing, it is always allowed adhesion on top of two different dimers and on top of a single dimer, blocking the dimers that arrive from higher layers to the lower layers due to overhangs (screening effects [8]).

Here, the calculation of the probability of percolation is performed using the burning algorithm [24], which is efficient when we need to know only if a particular configuration is a percolating one or not. The adsorption algorithm discussed above is implemented until the multilayer reaches a certain height, and thereafter we apply the burning algorithm to know if the configuration percolated or not. By repeating this process many times (around 12 000 times), we can build an approximate version of the percolation probability curve for each height.

The Frank and Lobb algorithm [25] was used for finding the conductivity between the left and right borders of the two-dimensional structure that results in the packing process of deposition of dimers. This procedure uses the repeated application of a sequence of transformations [series, parallel, and star delta $(Y - \Delta)$] to the bonds of the lattice. The final result of this sequence of transformations is the reduction of any finite portion of the lattice to a single bond that has the same conductance as the entire lattice. Before applying the algorithm of Frank and Lobb, we prepare the square lattice as follows. After the adsorption of dimers up to a certain maximum height [e.g., resulting in the packed structure of Fig. 1(a), for $L = 8$ and $H_{\max} = 3$], there will be three types of connections between neighbors. In the horizontal direction, two neighboring sites can be interconnected by (i) the same dimer or different dimers—this connection will have a resistance R_1 [black resistor in Fig. 1(b)]—and (ii) one dimer and one empty site or two empty sites—this connection would have a resistor R_3 [white resistor in Fig. 1(b)]. In the vertical direction, the connections between neighboring sites could be between two dimers of adjacent layers—in this case, the connection would have a resistance R_2 [gray resistor in Fig. 1(b)] or between a dimer and one empty site or two empty sites—in this case, the connection would have a resistance R_3. The choice of these three parameters (R_1, R_2, and R_3) is not arbitrary since each one has a different physical meaning. R_1 and R_2 provide information about the local longitudinal and transversal components of the conductivity, respectively. The parameter R_3 samples the resistance of the dielectric medium that fills the empty space between the dimers.

Finite-size scaling analysis was carried out for obtaining the percolation probability $P_p = P_p(H_{\max}, L)$ and the conductivity $\sigma(H_{\max}, L)$ as $L \to \infty$. For this, we use the curve collapse method [26,27] to obtain the critical parameters. We assume that the percolation probability has the form

$$P_p(H_{\max}, L) = F[(H_{\max} - H_c)L^{\nu}], \tag{1}$$

were $F[]$ is the scaling function. The idea of the method is the minimization of the area between all pairs of the curves $F[(H_{\max} - H_c)L^{\nu}]$. We perform the automatic search in the discrete plane $[H_{c_i} : \Delta H_c : H_{c_f}; \nu_i : \Delta\nu : \nu_f]$, where $H_{c_i}(\nu_i)$ and $H_{c_f}(\nu_f)$ are the lower and upper limits, respectively, of $H_c(\nu)$ in the search, ΔH_c and $\Delta\nu$ are resolutions of the search and represent the errors of H_c and ν, respectively.

III. RESULTS AND DISCUSSION

In this paper, we are interested in the behavior of the transport properties (percolation and conductivity) of the two-dimensional structure resulting from the multilayer packing process as a function of the height of the multilayer.

A. Percolation

To visualize the amorphous structure formed during the packing process, in Fig. 2 we have shown typical multilayer packing configurations for the adsorption of dimers with the rules defined in Sec. II. We show typical packing configurations for five values of time $t = 3000$, 5000, 6000, 10 000, and 15 000 from bottom to top, respectively, for a one-dimensional substrate of $L = 800$. In this figure, the clusters (set of sites

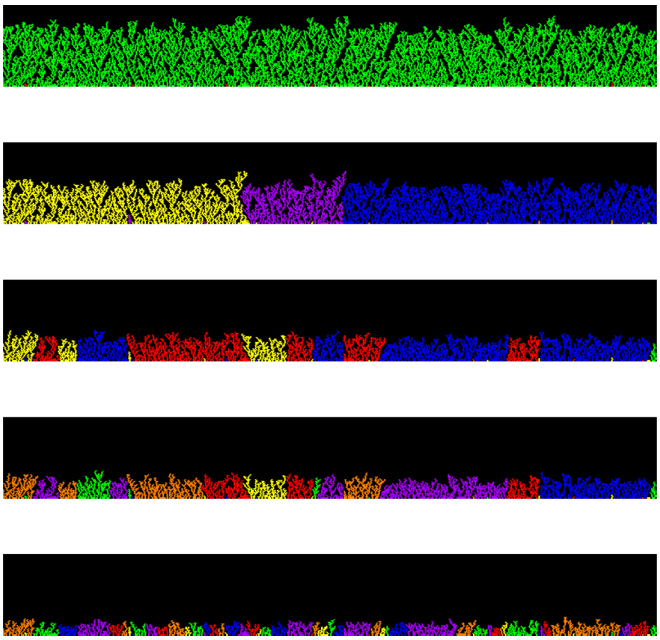

FIG. 2. Typical multilayer packing configurations for the adsorption of dimers for simulation time $t = 3000$, 5000, 6000, 10 000, and 15 000 from bottom to top respectively, for a one-dimensional substrate of $L = 800$. The different colors in the figure represent the clusters.

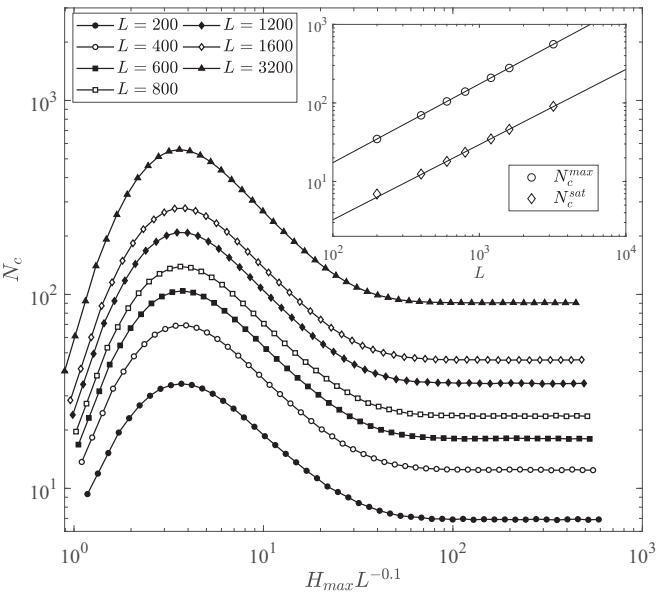

FIG. 4. Behavior of N_c as function of $H_{\max}$ for seven values of L. Inset: Scaling analysis of the function $N_c(L)$ in the maximum ($N_c^{\max}$) and before reaching the saturation (N_c^{sat}). See text for more details. In the main plot and in the inset, the size of the symbols is larger than the corresponding error bars.

interconnected through their neighboring sites) of adsorbed dimers are represented with different colors. Note that the clusters combine to form larger clusters with increasing simulation time, or what is the same, the height of the multilayer.

As can be verified in Fig. 3, the maximum height of the multilayer ($H_{\max}$) grows linearly with respect to the mean of simulation time. This can be analytically verified (without considering screening effects) from the mean-field model introduced by Ref. [8], specifically in Eq. (2.5). Our simulations report that the screening consideration maintains the linear behavior. Using the curve collapse method described in Sec. II, we find that $H_{\max}$ scales with the linear size of the substrate in the form $H_{\max} \sim L^{-0.986\pm0.003}$, as observed in the inset of Fig. 3.

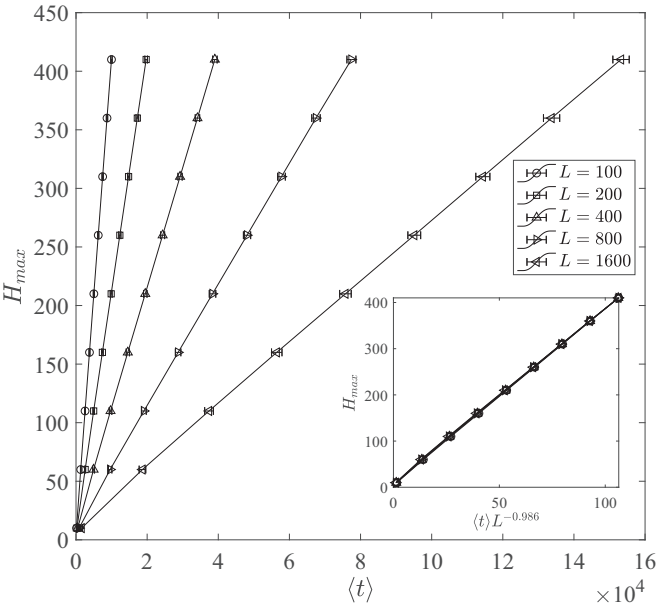

FIG. 3. Behavior of $H_{\max}$ with respect to the average simulation time to reach it, for five values of L. The horizontal bar errors represent the standard deviation. Inset: Curve collapse analysis for the data of the main plot.

In Fig. 4 (main plot), we show the behavior of the average cluster number N_c as a function of the height of the multilayer $H_{\max}$. Initially, during the packaging of the first layers (nucleation), the number of clusters increases until reaching a maximum value $N_c^{\max}$. At this point, no new clusters are created and a union process of the existing clusters (growth) hardly occurs, leading to a decrease in the number of clusters. As expected, for a sufficiently large height there will be only one cluster connecting the two faces (left and right), that is, the percolation cluster—this is equivalent to a saturation of the number of clusters in a value N_c^{sat}.

An anomalous scaling can be identified in the function $N_c(H_{\max}, L)$ since it seems to present two types of scaling. Based on the inset in Fig. 4, it can be identified, using a linear fit represented by solid lines, that the region of the maximum of the curves scales in the form $N_c^{\max} \sim L^{1.002\pm0.003}$ and the region of saturation in the form $N_c^{\text{sat}} \sim L^{0.957\pm0.036}$; the errors represent a 95% confidence bounds. Note that in Fig. 4, the horizontal axis was multiplied by the scale factor $L^{-0.1}$ so the maximum of all the different curves collapse in the same abscissa. At this point, it is interesting to note that N_c is a locally convex function in the neighborhood of $N_c^{\max}$, which bears some analogy with entropy, an aspect that is confirmed by the fact that N_c exhibits linear scaling with L, that is, manifesting the extensive property of entropy for a one-dimensional system.

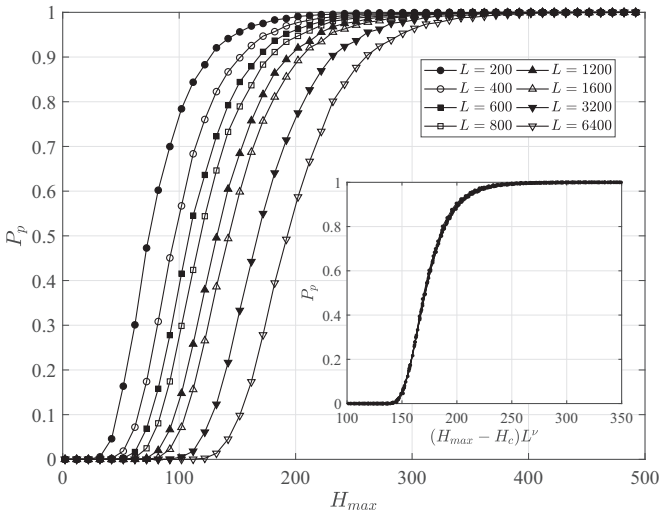

FIG. 5. Percolation probability as function of the height of the multilayer. Inset: Collapse of the percolation probability curves for $H_c = -213.2 \pm 0.1$ and $\nu = -0.099 \pm 0.001$.

The most important question here is, What is the probability that the system percolates for a given maximum height of the multilayer? In other words, we must calculate the probability P_p that, given a value of $H_{\max}$, there exists a spanning cluster of adsorbed dimers. The percolation probability P_p versus the height of the multilayer was obtained for linear size $L = 200$, 400, 600, 800, 1200, 1600, 3200, and 6400 and the number of runs is 12 000 for each $H_{\max}$ (Fig. 5).

By applying the method of curve collapse previously described (see Sec. II) for the simulation data in the main plot of Fig. 5, we obtained the corresponding results shown in the inset. A good collapse of the data occurs for the critical parameters $H_c = -213.2 \pm 0.1$ and $\nu = -0.099 \pm 0.001$, where the errors represent the resolution used when applying the curve collapse method. The percolation threshold H_c for a given lattice size L can be estimated from the condition $P_p(h_c, L) = 0.5$. With the collapsed curves, it is simple to estimate the percolation threshold in the thermodynamical limit $L \to \infty$ from the condition $P_p[h_c = (H_{\max} - H_c)L^{\nu}] = 0.5$. So, from the inset in Fig. 5 we can conclude that $h_c \simeq 171.5 \pm 2.3$. Here, the error was estimated by measuring the width of the bundle of curves when intersecting the horizontal line $P_p = 0.5$ in the inset of Fig. 5.

Note that in this system it is intuitive to think that the saturation of the number of clusters (see Fig. 4) is a signal that the system percolates (with probability $P_p = 1$, see Fig. 5). In other words, if the number of clusters does not vary, it means that there is only one percolation cluster obstructing any passage of dimers to the lower layers, so all dimers that arrive after saturation will necessarily belong to the percolation cluster. Our results show (see Fig. 4) that the number of clusters at saturation also increases approximately linearly with L, this translates into a proportional shift to the right in the P_p curves.

B. Electrical conductivity

The calculations of the conductivity σ were performed for each time until the multilayer reaches a given height. For each given value of $H_{\max}$, the computer experiments were repeated 12 000 times. In Fig. 6(a), we show the behavior of the conductivity σ as a function of the height of the multilayer. In Fig. 6(a), for each value of $H_{\max}$, all 12 000 replicas values are plotted without averaging (gray points) and the solid line represents the mean. The values of the internal resistors are $R_1 = R_2 = 1$ and $R_3 = 10^8$.

As expected from critical phenomena, the system presents two states, i.e., high and low conductivity [see Fig. 6(a)]. The jump between these states occurs close to the percolation threshold (critical height H_c). Below H_c, the probability of percolation is very low and few replicas contribute to the conductivity of the lattice. For heights greater than H_c, the probability of percolation is greater, which implies that many replicas will contribute to higher conductivity values. Near the percolation threshold, the fluctuations are large because the probabilities of percolating or not are very similar [see the second frame of Fig. 6(b)] and therefore the system is frustrated.

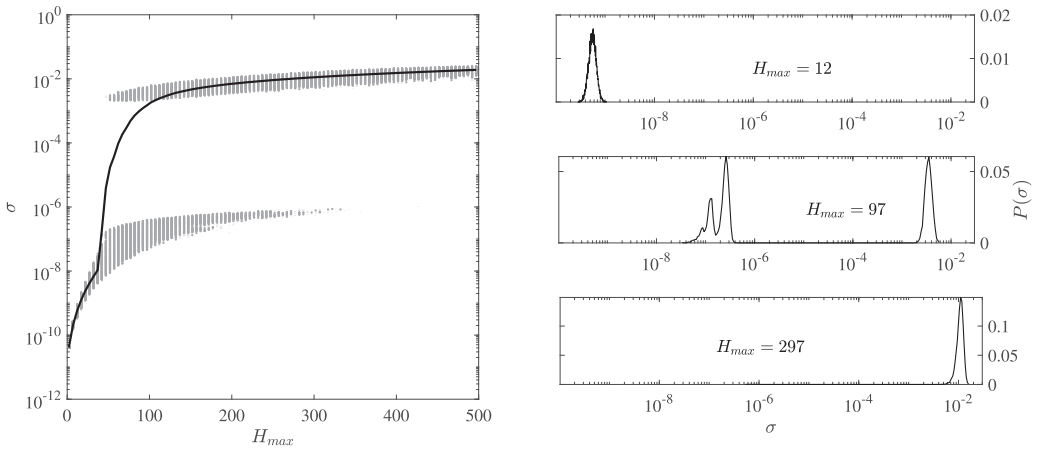

FIG. 6. (a) Plot of all replicas (12 000) of numerical experiments to determine σ for each value of $H_{\max}$. (b) Estimation of the probability of σ for different values of $H_{\max}$. Both results [(a) and, consequently, (b)] are obtained from a substrate with size $L = 500$.

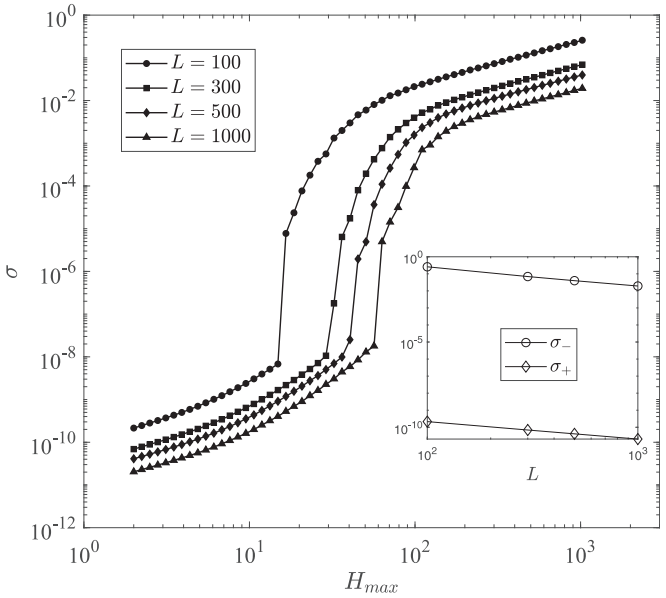

FIG. 7. Mean conductivity as a function of $H_{\max}$ for different values of L. Inset: Scaling analysis of conductivity $\sigma_{-(+)}$ before (after) the percolation transition. In the main plot and in the inset, the size of the symbols is larger than the corresponding error bars.

This means that many replicas must be taken to guarantee a smooth behavior of the mean curve of the conductivity [solid line in Fig. 6(a)].

The existence of two states leads to a bimodal distribution for the conductivity, whose modes represent the mean values of each conductivity state for each value of $H_{\max}$ [see Fig. 6(b)]. Figure 6 reflects other interesting features of the system. It can be shown that the width of the gap that separates the most probable values of the distribution $P(\sigma)$ is directly related to the difference between the values of $R = R_1 = R_2$ and R_3. Other simulations were made (not shown in the current paper) with different values of R and R_3 and we verify that the scaling properties, studied next, do not change significantly.

In Fig. 7, we show the scaling analysis for the mean conductivity as a function of $H_{\max}$ for four values of L.

In two-dimensional single-layer systems, it is well-known that the conductivity σ near the percolation threshold obeys different scaling relations for σ_- (the conductivity before the percolation transition) and σ_+ (the conductivity after the percolation transition) [28]. A study of the finite size effects for our model is presented in the inset of Fig. 7 to discuss the universality class of the phase transition the system undergoes [18]. From the linear fit, we can conclude that the pretransition and post-transition conductivities obey the scaling laws $\sigma_- \sim L^{-1.02\pm0.03}$ and $\sigma_+ \sim L^{-1.13\pm0.25}$ regardless of the value of $H_{\max}$ as long as it is far enough from the transition region. The errors represent 95% confidence bounds. In the case of Ref. [18], the scaling exponents for σ_+ and σ_- are equal in modulus with a value close to 0.975; being close to the values found in our paper, i.e., 1.02 (within 5% uncertainties) for σ_-, but they depart from our value 1.13 (within 16% uncertainties) for σ_+. Although the values of the exponents found here and those of Ref. [18] do not necessarily have to be the same, because the physical processes studied are different, the proximity between them suggests, in principle, that they can perhaps be accommodated in the same class of universality.

IV. CONCLUSION

Here we introduced a model of amorphous disordered matter of theoretical and applied interest obtained with the random juxtaposition of dimers. The deposition of dimers is based on an application of the widely known irreversible RSA algorithm. It occurs along one-dimensional substrates forming two-dimensional percolating multilayered structures that are investigated here in detail for the first time. The model exhibits critical properties for the emergent electrical conductivity that depends on three parameters able to describe a plethora of physical behaviors. A number of variants of the process studied here, such as the existence of competition between different species to be adsorbed and the inclusion of temperature effects, leading to the possibility of failures in the irreversible adsorption, can be introduced to describe more realistic processes for various specific purposes.

ACKNOWLEDGMENTS

G.P. thanks a fellowship from Conselho Nacional de Desenvolvimento Científico e Tecnológico (CNPq) Process No. 381191/2022-2. L.A.P.S. acknowledges CNPq for Grant No. 305017/2021-7. M.A.F.G. acknowledges financial support from the Brazilian Agency CAPES PROEX 23038.003069/2022-87, No. 0041/2022.

[1] A. Rényi, On a one-dimensional problem concerning random space-filling, Publ. Math. Inst. Hung. Acad. Sci. **3**, 109 (1958).

[2] V. Privman, H. Frisch, N. Ryde, and E. Matijević, Particle adhesion in model systems. Part 13. Theory of multilayer deposition, J. Chem. Soc., Faraday Trans. **87**, 1371 (1991).

[3] V. Privman, N. Kallay, M. Haque, and E. Matijevć, Magnetic effects in particle adhesion. Part III. Magnetite particles on steel, and glass, J. Adhes. Sci. Technol. **4**, 221 (1990).

[4] H. Gao, W. Xu, M. Li, N. Ilyas, J. Wang, W. Li, and X. Jiang, Hyperbolic metamaterials based on multilayer Ag/TiNxOy structure for SPR refractive index sensors, Opt. Laser Technol. **151**, 108034 (2022).

[5] X. Lü, X. Meng, Y. Shi, H. Tang, and W. Bao, Multilayer microstructured high-sensitive ultrawide-range flexible pressure sensor with modulus gradient, IEEE Trans. Electron Devices **69**, 2030 (2022).

[6] M. Ni, J. Chen, C. Wang, Y. Wang, L. Huang, W. Xiong, P. Zhao, Y. Xie, and J. Fei, A high-sensitive dopamine electrochemical sensor based on multilayer Ti_3C_2 MXene, graphitized multi-walled carbon nanotubes, and ZnO nanospheres, Microchemical J. **178**, 107410 (2022).

[7] R. Peña-Garcia, A. Delgado, Y. Guerra, and E. Padrón-Hernández, YIG films with low magnetic damping obtained by solgel on silicon (100), Mater. Lett. **161**, 384 (2015).

[8] M. Bartelt and V. Privman, Kinetics of irreversible multilayer adsorption: One-dimensional models, J. Chem. Phys. **93**, 6820 (1990).

[9] S. Yang, P. Viot, and P. Van Tassel, Generalized model of irreversible multilayer deposition, Phys. Rev. E **58**, 3324 (1998).

[10] P. Parida and H. Dhillon, Multilayer random sequential adsorption, J. Stat. Phys. **187**, 1 (2022).

[11] A. I. Gubanov, *Quantum Electron Theory of Amorphous Conductors* (Springer Science and Business Media, New York, NY, 1965).

[12] E. Ping, *Electronic, and Photonic Devices: Experimental Investigations of Hydrogenated Amorphous Silicon Substrate Solar Cell, and Fundamental Properties of Quantum Wells with Cylindrical Geometry, and Applications to Electronics, and Photonics* (Iowa State University, Ames, IA, 1995).

[13] L. Kazmerski, *Polycrystalline, and Amorphous Thin Films, and Devices* (Elsevier, 2012).

[14] W. G. J. H. M. Sark, L. Korte, and F. Roca, *Physics, and Technology of Amorphous-Crystalline Heterostructure Silicon Solar Cells* (Springer Science & Business Media, Berlin, Heidelberg, 2012).

[15] Y. Tarasevich, V. Goltseva, V. Laptev, and N. Lebovka, Electrical conductivity of a monolayer produced by random sequential adsorption of linear k-mers onto a square lattice, Phys. Rev. E **94**, 042112 (2016).

[16] Y. Tarasevich, V. Laptev, V. Goltseva, and N. Lebovka, Influence of defects on the effective electrical conductivity of a monolayer produced by random sequential adsorption of linear k-mers onto a square lattice, Physica A **477**, 195 (2017).

[17] S. Kundu, H. Prates, and N. Araújo, Jamming, and percolation in the random sequential adsorption of a binary mixture on the square lattice, J. Phys. A: Math. Theor. **55**, 204005 (2022).

[18] V. Cherkasova, Y. Tarasevich, N. Lebovka, and N. Vygornitskii, Percolation of aligned dimers on a square lattice, Eur. Phys. J. B **74**, 205 (2010).

[19] B. V. Derjaguin, N. V. Churaev, and V. M. Muller, *Surface Forces* (Springer Science and Business Media, New York, NY, 1987).

[20] D. Langhe and M. Ponting, *Manufacturing, and Novel Applications of Multilayer Polymer Films* (William Andrew, 2016).

[21] A. Jordan, B. Lee, K. Kim, E. Ludtke, O. Lhost, S. Jaffer, F. Bates, and C. Macosko, Rheology of polymer multilayers: Slip in shear, hardening in extension, J. Rheol. **63**, 751 (2019).

[22] M. Crescimanno, G. Mao, J. Andrews, K. Singer, E. Baer, A. Hiltner, H. Song, K. Comeau, B. Shakya, and A. Bishop, Others role of group velocity delay in Faraday rotation in a multilayer polymer lattice, JOSA B **29**, 1038 (2012).

[23] P. Petroff, A. Cho, F. Reinhart, A. Gossard, and W. Wiegmann, Alloy Clustering in $Ga_{1-x}Al_{xAs}$ Compound Semiconductors Grown by Molecular Beam Epitaxy, Phys. Rev. Lett. **48**, 170 (1982).

[24] H. Herrmann, D. Hong, and H. Stanley, Backbone, and elastic backbone of percolation clusters obtained by the new method of 'burning', J. Phys. A: Math. Gen. **17**, L261 (1984).

[25] D. Frank and C. Lobb, Highly efficient algorithm for percolative transport studies in two dimensions, Phys. Rev. B **37**, 302 (1988).

[26] S. Bhattacharjee and F. Seno, A measure of data collapse for scaling, J. Phys. A: Math. Gen. **34**, 6375 (2001).

[27] G. Palacios, and M. A. F. Gomes, Random sequential adsorption on non-simply connected surfaces, J. Phys. A: Math. Theor. **53**, 375003 (2020).

[28] D. Stauffer and A. Aharony, *Introduction to Percolation Theory* (Taylor and Francis, London, 1992).